

Preprint Manuscript

Bridgelall, R., and Tolliver, D. (2021). Railroad Accident Analysis Using Extreme Gradient Boosting. *Accident Analysis and Prevention*, 156(2021). DOI: 10.1016/j.aap.2021.106126, 2021(106126).

1 **Railroad Accident Analysis Using Extreme Gradient Boosting**

2 **Raj Bridgelall, Ph.D.**, Corresponding Author

3 Assistant Professor, Department of Transportation, Logistics & Finance

4 College of Business, North Dakota State University

5 Fargo, ND 58108; Email: raj@bridgelall.com, ORCID: 0000-0003-3743-6652

6

7 **Denver D. Tolliver, Ph.D.**

8 Director, Upper Great Plains Transportation Institute, North Dakota State University

9 Fargo, ND 58108; Email: denver.tolliver@ndsu.edu, ORCID: 0000-0002-8522-9394

10

11 Declarations of Interest: None.

12

13

35 **1 Introduction**

36 U.S. railroads have been an important driver of economic progress for more than 150 years.
37 Today, U.S. railroads carry approximately one-third of the nation's exports [1]. Therefore, the
38 safe and efficient operation of railroads is crucial to the nation's economic health. Unfortunately,
39 railroads lose hundreds of millions of dollars from accidents each year. Analysis of the Federal
40 Railroad Administration (FRA) Rail Equipment Accident database revealed that human-factors
41 was consistently the dominant cause of railroad accidents [2]. Hence, the federal government
42 mandated that railroads deploy a positive train control (PTC) system by 2018 to help prevent
43 accidents caused by human errors [3]. With PTC now in place, it is important for analysts to
44 study other common causes of accidents.

45 The **goal** of this research is to identify factors associated with the most frequent and
46 expensive types of accidents that are not attributable to human error. Data mining of FRA
47 accident records from January 1, 2009, to June 30, 2020, revealed that derailment accidents
48 accounted for 70.9% of the average annual financial loss (Figure 1). The trend showed that
49 derailment accidents maintained a steady rate each year. Therefore, the ability to identify and
50 rank features that increase the risk of derailments over other accident types can inform more
51 cost-effective and impactful risk management strategies.

52 An **objective** of this research is to build a supervised machine learning (ML) model that can
53 predict derailments from other accident types and to rank the importance of those features that
54 contribute towards the classification accuracy. However, no single type of ML model performs
55 best on all types of datasets. Therefore, another objective is to compare the classification
56 performance of various types of ML models on the same dataset.

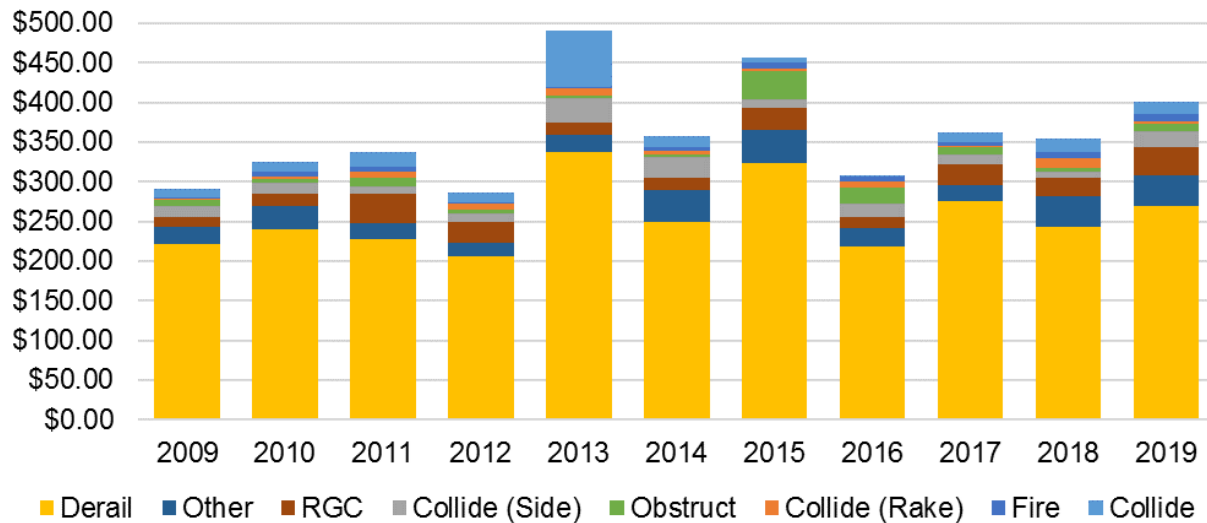


Figure 1: Annual financial loss reported for different accident types.

57
58

59 One of the main challenges in data science is to effectively clean datasets before using them
60 to train ML models. Studies estimate that dirty data costs the U.S. economy trillion of dollars
61 each year [4]. A survey of data cleaning for ML found that the failure to discover and repair dirty
62 data can weaken data analysis techniques [5]. Although a few approaches to data cleaning are
63 common, every dataset poses unique challenges [6]. Hence, data scientists spend an average of
64 60% of their time cleaning and organizing data [4].

65 Although the importance of using clean data is well-known, the research community has paid
66 little attention to the advancement of data cleaning techniques [7]. The most commonly used
67 techniques are those that detect and remove outliers and duplicate records [4]. Even so, those
68 techniques alone cannot effectively clean all types of datasets. Other techniques that can find
69 data entry errors use customized rules to detect violations, for example, house prices exceeding
70 an expected range for a given neighborhood. Custom techniques tend to be heuristic, so they
71 require good familiarity with the data and its meaning. Considering the challenges outlined
72 above, the following are **contributions** of this research:

- 73 • A customized framework to clean a relevant subset of the FRA database and to fill 100%
74 of missing values for the important attributes (Section 3.1).
- 75 • Brief explanations of how each ML method works to gain understanding about the
76 impact of their hyperparameter tuning (Section 3.2).
- 77 • Importance ranking of the feature relevance in predicting accident type (Section 3.3).
- 78 • Visualizing and interpreting the classification power of each attribute by principle
79 component analysis (PCA) to gain insights about the performance differences among the
80 ML models evaluated (Section 3.4).

81 The next section (Section 2) reviews related works and their findings in relation to the
82 contributions of this research. Section 4 mirrors the methods section to present the results.
83 Section 5 discusses the significance and interprets the outcome. Section 6 recaps the findings and
84 concludes with how future research can leverage the methods of this research to further the
85 agenda in accident analysis.

86 **2 Related Works**

87 Studies that use ML methods to analyze accidents are more common for roadways than for
88 railroads. For example, Iranitalab and Khattak (2017) compared the performance of Multinomial
89 Logit (MNL), k-Nearest Neighbor (kNN), Support Vector Machines (SVM) and Random Forests
90 (RF) in predicting the crash severity of two-vehicle roadway crashes [8]. They found that kNN
91 and MNL had the best and worst performance, respectively, when applied to crash data from
92 Nebraska, United States. A recent survey of big data analytics applied to railroads found that of
93 115 journal articles reviewed from 2003 to 2017, only 22% covered railroad safety whereas 49%
94 and 29% covered maintenance and operations, respectively [9]. This imbalance suggests that the

95 research community and the railroad industry can benefit from additional analysis of railroad
96 accident risks.

97 Several studies used ML techniques to analyze highway-rail grade crossing (HRGC)
98 accidents. Dabbour et al. (2017) applied ordered regression models to HRGC crash data and
99 found that higher train and vehicle speeds were positively correlated with driver injury severity
100 [10]. Liu and Khattak (2017) applied geospatial modeling to HRGC crash data and found that
101 gate violations were more highly associated with two-quadrant than four-quadrant gates [11].
102 Karamati et al. (2020) applied random survival forest to HRGC crash data and found that adding
103 audible alarm devices to crossings that already have gates and flashing lights can decrease crash
104 likelihood by approximately 50% [12]. Soleimani et al. (2019) used extreme gradient boosting to
105 identify HRGCs that should be closed to prevent accidents [13]. Wali et al. (2021) applied text
106 mining to crash narrative data of railroad trespassing incidents and found that confirmed suicide
107 attempts and the use of headphones or cellphones were more likely to result in fatal injuries [14].

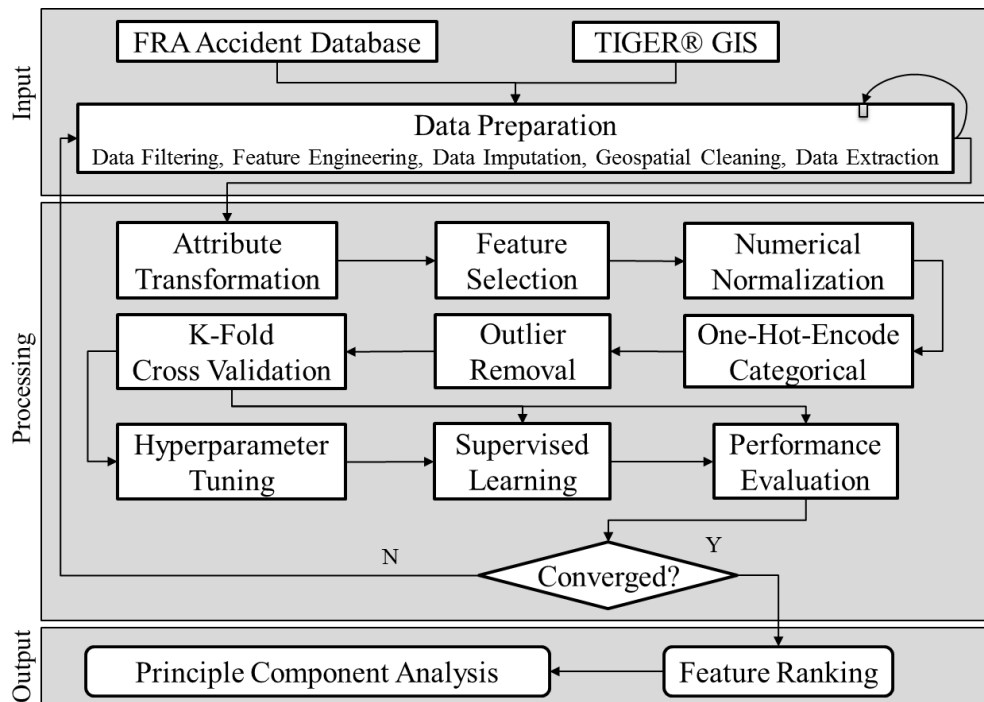
108 Only a few studies focused on derailment-type accidents. Liu et al. (2017) found that
109 derailment rates on Class 1 railroad mainlines were lower for signalized tracks with higher FRA
110 track class and higher traffic density [15]. Wang et al. (2020) found that most derailment type
111 accidents declined with the greatest reductions in broken rails, irregular track geometry, and
112 wheel-related equipment defects [16]. Iranitalab and Khatta (2020) found that the random forest
113 method of ML outperformed the logistic regression, Naïve Bayes, and support vector machine
114 (SVM) methods in classifying train-level hazmat releases with an AUC score of 87% [17].

115 The survey of Ghofrani (2018) demonstrated that researchers have also use ML methods to
116 analyze other aspects of railroad operations besides safety [9]. For example, Li et al. (2014) used
117 ML to learn rules from historical and real-time data to predict railroad maintenance needs [18].

118 Lasisi and Attoh-Okine (2019) proposed a combination of ensemble tree-based ML models to
 119 predict rail fatigue defects and achieved an AUC score of 0.783 [19].

120 3 Methodology

121 Figure 2 shows the methodological framework developed to prepare the data, apply the machine
 122 learning methods, rank the features, and to interpret the results.



123 Figure 2: The methodological framework.
 124

125 The next two subsections cover each procedure shown in the input, processing, and output layers
 126 of the framework. The input layer gathers the datasets and prepares the combined data by
 127 applying various methods to reduce noise, repair data entry errors, and fill in missing values. The
 128 processing layer prepares relevant attributes to train and tune the ML models. The ML process
 129 itself resulted in the discovery of additional errors that the data preparation layer subsequently
 130 addressed. The looping converged after the ML performance stabilized. The final layer ranked
 131 the importance of attributes in classification performance and used PCA to visualize the results
 132 for interpretation.

133 **3.1 Data Preparation**

134 Erroneous data or attributes that have no influence in deciding the target class (derailment versus
135 non-derailment) become noise and diminish the predictive performance of ML models. Missing
136 or low dispersion data can increase model bias. The next subsections describe some customized
137 data cleaning and imputation methods that this research developed for the FRA dataset.

138 **3.1.1 Data Filtering**

139 “Big data” is often associated with what the literature calls a “curse of dimensionality” where
140 each additional attribute exponentially increases the volume of the feature space to a point where
141 the data becomes too sparse to be statistically significant or to have any structure [20]. Therefore,
142 methods to identify and remove irrelevant attributes or features can increase the cohesiveness
143 and quality of the dataset. Table 1 describes criteria used to eliminate irrelevant attributes or
144 features.

145 Table 1: Criteria for Attribute or Feature Elimination

Criteria	Description
Sparsity	Attribute is missing more than 85% of the values.
Duplication	Attribute contains the same information as other attributes.
Sparsity	More than 85% of the attribute contain zeros.
Correlated	Attribute is more than 90% correlated with another.
Redundancy	Attribute contains information that is inherent in other attributes.
Noise	Attribute is not relevant to the target class.
Dispersion	Attribute has low variance or carries little or no information.
Combinable	Attribute that can combine with others without losing information.

146

147 **3.1.2 Feature Engineering**

148 The manipulation of features to improve ML model performance is more art than science
149 because there are no automated or standardized techniques for all types of datasets [20]. The
150 effectiveness of feature engineering requires in-depth knowledge of the dataset, its structure, and
151 the meaning and significance of each attribute. The empirical feature engineering was conducted
152 as follows:

- 153 1) Packaged similar features of an attribute to simplify the categories.
- 154 2) Converted categorical attributes that have some ranking to ordinal attributes.
- 155 3) Binarized categorical attributes that contained only two values by replacing one value
156 with zero and the other with one.
- 157 4) Replaced nominal values with a single word label to enhance the ease of interpreting
158 trends with more descriptive legends.

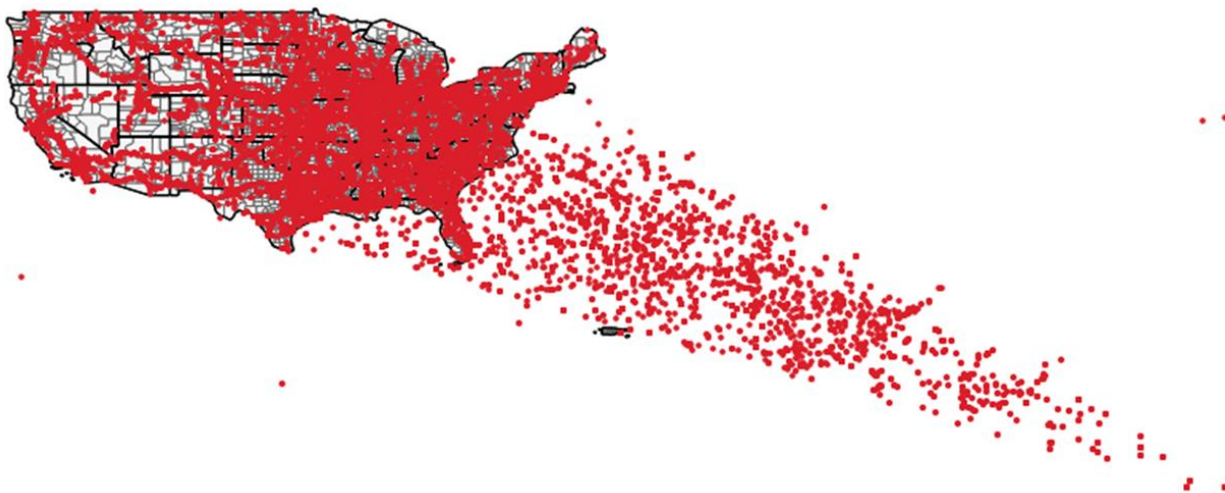
159 **3.1.3 Data Imputation**

160 A few methods such as decision trees and Bayesian classifiers can work with missing data, but
161 most cannot [21]. Therefore, data scientists developed a few methods to impute or guess missing
162 values. Common approaches are to replace missing values with the mean, median, most frequent,
163 random, or zero value. More intelligent approaches use tree-based ML techniques to fill missing
164 values with those of their nearest neighbors. This research developed a new method, dubbed
165 *local association pivot* (LAP), to replace missing values. The LAP method first creates a pivot
166 table that aggregates non-missing values by a location identifier and by sub-location identifiers if
167 available. The method then merges the pivot table with the dataset by using the main location
168 identifier as the unique merge key. The aggregation method for the pivot depends on the type of
169 missing data. For example, for numerical values such as track density, the method used the
170 maximum of the aggregated value for a location. The method did not use the average value
171 because zero or missing values created an undesirable bias in the aggregation. A fringe benefit of
172 using the LAP method is that it is easy to spot data entry or spelling errors by examining a sorted
173 list of the unique location keys.

174 **3.1.4 Geospatial Cleaning**

175 Missing or erroneous geospatial coordinates are impossible to impute or correct if no other
176 spatial information is available in the dataset. The state or county name provides a coarse
177 location identifier that can be helpful for visualizing data on maps. However, a coarse location
178 such as a large state may introduce bias in the ML process. Fortunately, the FRA database
179 contains the station name that is closest to the accident location, so its location can be a surrogate
180 for missing geospatial coordinates.

181 Aside from missing geospatial coordinates, data entry errors may result in erroneous or
182 highly skewed geospatial locations. Figure 3 shows the positions of the recorded geospatial
183 coordinates relative to a map of the continental United States. There is an observable systematic
184 skew towards the southeast. This skew suggests that there was a lack of resolution for those
185 coordinates because in North America, lower resolution latitude and longitude coordinates would
186 bias towards the south and east, respectively.



187
188 Figure 3: Positions of the recorded geospatial coordinates in the FRA database.

189 The procedure to clean the geospatial coordinates filled missing values in two stages. First, the
190 LAP method averaged the non-missing geospatial coordinates for accidents that occurred on a
191 given track type near a given station. Second, the procedure merged the records with a map file

192 from the U.S. Census Bureau TIGER® database that contained the geospatial centroid of each
193 county in the United States. A geographic information system (GIS) spatial join method then
194 replaced erroneous geospatial coordinates as follows:

- 195 1. Spatially join the TIGER county polygons to the FRA geospatial coordinates using one-
196 to-many mapping. This procedure added the county FIPS code from the TIGER database.
- 197 2. Flag any mismatch between the reported FRA county FIPS code and the spatially joined
198 county FIPS code by a Boolean flag MATCH. This flag identified geospatial coordinates
199 that were not located within the FRA county recorded for the accident.
- 200 3. Replace the geospatial coordinates of the flagged records with the geospatial centroid of
201 the FRA reported county.

202 A clear limitation of the LAP method is that it reduces the geospatial error by a small amount.

203 However, the error reduction helps the ML performance without forcing data elimination.

204 ***3.1.5 Data Extraction***

205 A consistent dataset improves ML performance [20]. The FRA dataset contained records of both
206 passenger and freight train accidents. Passenger trains operate in environments and
207 circumstances that are often different from those of freight trains. For example, passenger
208 terminals and stations are different from freight and transshipment terminals. Hence, equipment
209 and operations are different for the two types of service. Passenger trains accounted for a small
210 portion 8.03% (2,354) of accidents from 2009 to July 31, 2020. Removing those records not only
211 enhanced the consistency of the dataset, but also removed a few attributes that were associated
212 with passenger trains only.

213 The FRA database codes the cause of an accident in the “ACCAUSE” attribute and cross-
214 referenced the description in Appendix C of the accident dictionary [22]. The document lists 389

215 accident-cause codes. The first character of the code indicates the accident cause category as “E”
216 for “Mechanical and Electrical Failures, “T” for “Rack, Roadbed and Structures,” “S” for
217 “Signal and Communication,” “H” for “Train operation – Human Factors,” and “M” for
218 miscellaneous causes that do not fit into any of the other categories. Therefore, the procedure
219 removed records for accidents due to human factors by extracting those where the first character
220 in the cause-code was not “H.”

221 ***3.1.6 Attribute Transformation***

222 ML algorithms tend to perform poorly on data with attributes that have a highly skewed
223 distribution because the model could treat data in long tails as outliers or because extreme values
224 provide insufficient examples [23]. This phenomenon is common, for example, in the
225 distribution of annual income (right skew) and the distribution of age at natural demise (left
226 skew). A standard technique is to log transform continuous attributes with highly skewed
227 distributions, including the target attribute if applicable. Using the shifted natural logarithm
228 $\text{LN}(1 + x)$ prevents an undefined number if attribute value x is zero.

229 Another transformation that can help to reduce the dimension of a dataset is to replace a set
230 of related attributes with proportions of a base attribute. The advantage of a proportion
231 transformation is that it retains information about the relative relationship among attributes while
232 normalizing the values within the $[0, 1]$ range. The attributes selected for this transformation
233 were the proportion of cars that contained freight (LOADF1), and the proportion of loaded cars
234 that contained hazardous materials (CARS).

235 It is also possible to increase the information of an attribute by making explicit some
236 knowledge that is within context of another attribute. For example, transforming the absolute
237 train speed with the excess speed, relative to the speed limit for the track class, increases

238 information for that attribute. Finally, attributes that are irrelevant but provide descriptive value
239 can store metadata instead of features to enhance further exploratory data analysis.

240 **3.1.7 Feature Selection**

241 Predictive modeling should not contain attributes where values are known only after the
242 outcome. Therefore, the cleaning procedure must eliminate *post-event* attributes such as the
243 number of people injured, killed, or evacuated. Other post-event attributes include the position of
244 involved equipment, the number of damaged vehicles, and the cause of the accident.

245 **3.1.8 Attribute Normalization**

246 Most ML algorithms work only with numerical data. Categorical attributes contain a finite
247 number of unique labels that have no numeric value, nor do they represent an ordering or
248 ranking. Therefore, the framework applies *one-hot-encoding* to create new binary attributes that
249 represent each category or feature of the attribute where “1” and “0” denotes presence or
250 absence, respectively. Unfortunately, one-hot-encoding grows the dimension of the ML dataset.
251 Therefore, any opportunity to reduce the number of categories in an attribute can alleviate the
252 curse of dimensionality. In this analysis, domain knowledge about the meaning behind the data
253 helped with packaging some of the categories of a few attributes into fewer groups that were also
254 more meaningful.

255 The performance of many ML algorithms improves when attributes become comparable by
256 normalization, which is to scale them to the same value range. The ML framework uses [0, 1]
257 normalization to make the magnitude of continuous variables comparable with one-hot encoded
258 categorical features. The transformation is

$$\hat{x} = \frac{x - \min x}{\max x - \min x} \quad (1)$$

259 where \hat{x} is the transformation of attribute value x .

260 **3.1.9 Outlier Removal**

261 Sacrificing a few outlier data points to reduce bias can improve the generalization of a model.

262 Outlier data instances are few and different from the bulk of the dataset [24]. They could

263 represent noisy data entries or rare events that can bias the training of an ML model, resulting in

264 poor predictive performance. Several outlier detection methods are available. The framework

265 used four methods to compare their effect on the model performance:

- 266 • One class SVM (OCS) with a radial basis function (RBF) kernel (OCS-RBF)
- 267 • Covariance estimator (CE) [25]
- 268 • Local outlier factor (LOF) [26]
- 269 • Isolation forest (IF) [24]

270 OCS-RBF applies support vector machine (SVM) classification to assess the similarity of a data

271 instance to the core class. Consequently, OCS-RBF performs well on data that is not Gaussian

272 distributed because it does not assume normally distribute attributes. The CE method fits ellipsis

273 to clusters with central points to identify data instances that are far away, based on the

274 Mahalanobis distance measure. However, CE requires data with a Gaussian distribution. LOF

275 measures the local density of a data instance with respect to the local densities of its k-nearest

276 neighbors. A large deviation of the two local densities indicates that the data instance is isolated.

277 LOF works well with moderately high-dimension datasets because the distance computation

278 scales linearly. The method of IF uses the random forest classification algorithm to detect data

279 instances that are different from most of the data [24]. Outlier removal occurs after one-hot-

280 encoding because some of the algorithms utilize ML methods that work with numerical variables

281 only.

282 **3.2 Machine Learning**

283 Many different types of ML models emerged over the years, and each tend to behave differently
284 on different types of datasets [27]. The next subsections describe the different types of models
285 and their hyperparameter tuning to optimize performance on the FRA dataset.

286 **3.2.1 Supervised Classification Models**

287 Table 2 summarizes the 11 different types of ML models used in this analysis. The table
288 provides a brief description of how each algorithm works, their most important hyperparameters
289 (HP), their overall advantages (A) and disadvantages (D). The table groups the models into four
290 broader categories based on their underlying theory of operation: tree-based methods, statistical
291 models, decision boundaries, and learned functions. Numerous excellent books describe the
292 mathematics and theory of operations for each model; they are incorporated here by reference.
293 Géron (2017) discusses both the theory and practical implementation of decision tree (DT),
294 random forest (RF), AdaBoost (AB), logistic regression (LR), support vector machine (SVM),
295 stochastic gradient descent (SGD), and artificial neural network methods [28]. Jame et al. (2013)
296 discusses both the theory and practical implementation of Naïve Bayes (NB), k-nearest-
297 neighbors (kNN), and tree-based boosting methods [27]. Hastie et al. (2016) provides similar
298 coverage for all the models used in this analysis, including some key ML concepts such as
299 bootstrapping, boosting, bagging, and ensemble learning [29]. Murphy (2012) covers the various
300 methods from a more theoretical and probabilistic perspective [20].

301

302 Table 2: ML Models Compared

Type	Model	Algorithm & Hyperparameters	Advantages and Disadvantages
Tree-Based Methods	Decision Tree (DT)	Recursive tree node splitting to maximize the purity of sub-trees. HP: Minimum number of instances in leaves (N), and minimum size of subsets (S).	A: Simple to interpret and to visualize. Works with non-numerical categorical attributes. D: Tends to overfit, resulting in low predictive power on new data.
	Random Forest (RF)	Build many full trees for voting. Each tree grows from a bootstrapped dataset and a random subset of attributes. HP: Number of trees (N) and minimum size of subsets (S).	A: Offers the simplicity and intuition of decision trees but with less tendency to overfit, therefore, improves generalization on unseen data. D: Incomplete trees diminish insights that full trees might otherwise provide.
	AdaBoost (AB)	Sequentially build improved shallow trees for voting. HP: Number of estimators (N), learning rate (R), boosting algorithm, and regression loss function.	A: Selects only those features that improve predictive power, hence, reducing the computational burden for datasets with very large dimensionality. Less sensitive to overfitting. D: Sensitive to the presence of outliers and data with high incoherence.
	Extreme Gradient Boost (XGB)	A highly configurable version of gradient boosting. HP: Number of estimators (N), learning rate (R), maximum tree depth (S), loss function.	A: Improved performance over gradient boosting and more efficient. D: Sensitive to hyperparameter selection; requires manual intervention to achieve the best configuration for a given dataset.
	Gradient Boost (GB)	Sequentially build improved models that fit the errors of previous models. HP: Number of estimators (N), learning rate (R), maximum tree depth (S), loss function.	A: Efficient and good performance on large datasets; inherently supports missing values. D: Sensitive to hyperparameter selection but has fewer to tune than extreme gradient boosting.
Statistical Models	k -Nearest Neighbors (k -NN)	Determine the class of an instance based on the majority class of its k nearest neighbors. HP: Number of neighbors (k), distance method.	A: Method simplicity. D: Sensitive to a skewed class distribution. The computational intensity grows exponentially with the number of instances and attributes.
	Naïve Bayes (NB)	Applies Bayes theorem to determine the class probability, given probabilities of the observations. HP: None	A: Fast and simple method. D: Poor performance when attributes are not independent.
Decision Boundaries	Logistic Regression (LR)	Establish a decision boundary by using a logistic function to maximally separate classes. HP: Regularization function and strength (C), and probability threshold.	A: Inherits many of the advantages of linear regression; precisions are easy to make. D: Sensitive to noise in the data such as outliers and incorrectly classified instances. Model fitting may fail to converge if there are many highly correlated features.
	Support Vector Machine (SVM)	Establish a decision boundary by finding a multidimensional hyperplane to maximally separate classes. HP: Kernel type, cost (C), and regression loss (ϵ)	A: High accuracy with low computational complexity. D: Sensitive to noisy data and multidimensional planes that lack clear boundaries.
Learned Functions	Stochastic Gradient Descent (SGD)	An optimization technique that fits a linear multivariate function to the data. It works best when all features are scaled. HP: Loss function, learning rate method and parameters.	A: An efficient technique on large datasets. D: Sensitive to feature scaling; many hyperparameters; and the true minima may not be achieved because the gradient is only an approximation.
	Artificial Neural Network (ANN)	A weighted multilayer linear network that represents a function. HP: Hidden layer neurons (N), solver type, regularization parameter (α), number of iterations (I).	A: Accuracy improves with use and feedback about classification accuracy. D: Requires many training examples to improve classification accuracy.

304 3.2.2 *Hyperparameter Tuning*

305 Each model requires that the user select values for key parameters (hyperparameters) that affect
306 their performance. Tuning hyperparameters require incremental adjustments while observing a
307 performance metric. The optimization loop uses *k-fold cross validation* to maximize the model
308 *generalization* on the entire dataset while reducing any tendency towards *overfitting* or
309 *underfitting*. Models that have *regularization* parameters provide a means to balance the
310 unavoidable tradeoff between *bias* and *variance*, which improves generalization on unseen data.
311 James et al. (2013) provides an excellent description of the above ML terminologies and
312 concepts, so the book is incorporated here by reference [27].

313 The performance evaluation metric used was the area under the curve (AUC) of the receiver
314 operating characteristic (ROC). The AUC trends with hyperparameter value adjustments show
315 where each model achieved its best regularized performance. The ROC plots the true positive
316 (TP) rate against the false positive (FP) rate as a function of the class membership probability
317 [30]. Intuitively, AUC measures the power of a model to distinguish among classes in the target
318 attribute. An AUC score of 0.5 indicates that the model has no ability to distinguish among
319 classes of the target whereas a value approaching 1.0 indicates that the model offers a large
320 increase in TP rate for a small price of slightly increasing the FP rate.

321 The performance evaluation procedure also monitored the classification accuracy (CA),
322 precision (Pc), recall (Rc), and F1 scores. Table 3 describes each metric and summarizes their
323 advantages and disadvantages. All performance metric except the AUC was sensitive to class
324 imbalance in the dataset.

325 Table 3: Classifier Performance Metric

Metric	Description	Advantages	Disadvantages
CA	The proportion of predictions that were correct.	Simply calculation.	Sensitive to data imbalance where a no-skill classifier can appear to provide better performance by predicting the dominant class every time. For example, a no-skill classifier will score CA at 90% if the database labels 90% of the accidents as derailments.
Pc	The proportion of observations correctly predicted as positives (TP) to the total number of observations predicted as positives (TP + FP).	Measures the probability of mislabeling a negative sample as positive.	A bias towards the majority class can be misleading.
Rc	Measures the proportion of positive predictions (TP) to the total number of positive observations (TP + FN)	Measures the probability of correctly labeling all the positive observations.	A bias towards the majority class can be misleading.
F1	The harmonic mean of Pc and Rc, scaled from 0 to 1.	Measures the balance between precision and recall.	Less bias but as a function of Pc and Rc will retain some bias.
AUC	Area under the ROC curve that plots TP against FP as a function of class membership probability.	Removes biased scores for imbalanced datasets.	More complex calculation than a simple ratio. Requires the class membership probability for every prediction, which may not be inherently available from a model.

326

327 CA is one of the most often cited performance metric for ML classifiers. However, a high
 328 CA score can be misleading if the dataset has high class imbalanced. For example, a no-skill
 329 algorithm applied to a dataset with only 5% of the instances from one class and the rest from the
 330 other class will appear to have a 95% accuracy if it picks the dominant class for every prediction.
 331 Stratified sampling of both the training and testing datasets helps to reduce the imbalance [31].

332 **3.3 Feature Ranking**

333 Attributes that contain noisy, irrelevant, or redundant information can diminish the performance
 334 of ML methods [32]. Hence, data scientists developed various methods to score features based
 335 on the amount of information they contribute towards distinguishing the target classes. This
 336 section compares five methods that rank features based on the strength of their association with
 337 the classes in the target attribute. Table 11 provides a short description of each method and a

338 reference that provides details about their theory of operations. All methods work best with
 339 normalized attributes because their magnitudes become comparable. The diversity of methods
 340 result in some compensating for the weaknesses of the other; therefore, they do not provide
 341 identical rankings [33]. However, a strong correlation among rankings indicates that the top-
 342 ranking attributes do contribute most towards ML classification performance.

343 Table 11. Feature Ranking by Scoring Methods

Method	Description	Reference
ANOVA	Analysis of Variance (ANOVA) measures the difference between average values of a feature in different classes of the target, based on the F distribution.	Agresti (2018) [34]
Chi-Squared	Measures a dependency or association between the feature and the target class by using a chi-square statistic.	Wang et al. (2010) [33]
Information Gain	The expected amount of entropy reduction. A decrease in entropy (uncertainty) based on the presence of other features will increase information.	Yu and Liu (2003) [32]
Gain Ratio	Reduces the bias of Information Gain towards features that have many values by taking the ratio of Information Gain to the intrinsic information (entropy) of the feature.	Quinlan (1986) [35]
Gini Decrease	A measure of the inequality among values of a frequency distribution based on their statistical dispersion. A value of zero and one represents perfect equality and inequality, respectively, of the distribution of a feature within each target class.	Han et al. (2016) [36]

344

345 3.4 Principle Component Analysis

346 The method of principle component analysis (PCA) creates a set of new orthogonal basis
 347 vectors, each maximally spanning the dimensions of feature space, in the order of the data
 348 variance [37]. Each principle component (PC) is a linear combination of all *numerical* features in
 349 the dataset. Intuitively, the first two principle components form a plane in feature space that is
 350 *closest* to all the data instances, as measured by the Euclidean distance. Data clusters tend to
 351 form along the directions of maximum variance. Hence, attributes that most influence the
 352 formation of data clusters contribute to inherent structure in the data. The terminology used in
 353 the literature is that each PC “explains” some proportion of the total variance (information) in the

354 dataset. Features that are weak components of most PCs tend to be associated with noise in the
355 data. The framework evaluates the trend in proportion of the variance that each PC *explains* to
356 provide insights about the amount and location of noise in the dataset.

357 **4 Results**

358 The subsections of this section mirror those of the methodology to organize the presentation of
359 the results from applying the analytical framework described previously. The main procedures
360 are data preparation, machine learning, attribute ranking, and PCA.

361 **4.1 Data Preparation**

362 The following subsections describe the data filtering, feature engineering, data imputation,
363 geospatial data cleaning, data extraction, attribute transformation, feature selection, and outlier
364 removal.

365 **4.1.1 Data Filtering**

366 Some of the data schema became inconsistent after the FRA changed reporting requirements for
367 a few of the fields starting June 1, 2011. For example, the report added a field to indicate if the
368 accident occurred in a signalized territory. Hence, there was no entry for the “SIGNAL” field
369 prior to the switchover date. Similarly, a field indicating the method of operation (“MOPERA”)
370 replaced the “METHOD” field that encoded similar information. Consequently, 22% and 79% of
371 the data was missing in the “MOPERA” and “METHOD” fields, respectively. The accident
372 reporting form also added a field “SSB1” to indicate if the track was a continuously welded
373 (CWR) or other. Hence, the “SSB1” field was mostly empty prior to June 1, 2011. Merging
374 8,055 records from 2009 to 2011 with 21,242 records from 2012 to June 2020 produced a total of
375 29,297 records with 145 attributes. Table 4 chronicles each criterion used to reduce the number
376 of fields from 145 to 52.

377 Table 4: Chronicle of Dimension Reduction for 29,297 Records

Criteria	Attributes Removed	Count
Sparsity	19 with > 85% missing data (e.g. DUMMY1-DUMMY7).	145 - 19 = 126
Duplication	8 with duplicated information (e.g. IMO, IYR, MONTH, YEAR).	126 - 8 = 118
Sparsity	16 with > 90% zero-filled (e.g. CABOOSE1, EVACATE, MIDREM1)	118 - 16 = 102
Correlated	12 with > 90% correlation with other attributes (e.g. PASSINJ, PASSKLD)	102 - 12 = 90
Redundancy	7 that were redundant with others (e.g. CNTYCD, STATE, COUNTY)	90 - 7 = 83
Noise	6 with no relevance to the target (e.g. train number, car number)	83 - 6 = 77
Noise	6 with > 20% missing or no relevance to the target (e.g. ADJUNCT1, DIV)	77 - 6 = 71
Combinable	HUMANS = (engineers + firemen + conductor + brakemen), drop 4.	71 - 4 + 1 = 68
Correlated	EQATT (equipment attended) correlates with HUMANS, drop 1	68 - 1 = 67
Combinable	Combine 15 narrative fields into a single field (NARR), drop original 15.	67 - 15 + 1 = 53
Combinable	Fill missing MOPERA (method of operation) data with METHOD, drop 1.	53 - 1 = 52

378

379 **4.1.2 Feature Engineering**

380 Several categorical attributes contained labels that resulted in fewer stratifications when
 381 combined. For example, the type of consist (“TYPEQ”) contained 14 different labels to describe
 382 sub-categories of the following 6 equipment categories: a “Freight” train, any type of
 383 “Passenger” train, any type of “Locomotive,” any set of cars without locomotives (“Cars”), any
 384 type of equipment used for maintenance and other non-revenue service work (“Work”), and any
 385 type of equipment used to manage yard movements (“Yard”). Similarly, MOPERA (method of
 386 operation or movement authorization) contained 21 categories that were simplified into the
 387 following 5 broader categories of movement authorization: signaling (“Signal”), direct control
 388 (“Control”), restricted limit of movements (“Restrict”), block control for track segments
 389 (“Blocks”), and other types of movement authorization (“Not Main”) that were not on the main
 390 tracks.

391 The feature engineering procedure converted track class (“TRKCLAS”) to an ordinal
 392 attribute because it encodes speed limits. The FRA track class designation increases the speed
 393 limit for both freight and passenger trains in a non-linearly manner from Class 1 (10 mph)
 394 through Class 9 (200 mph), which the ordinal encoding from 1 through 9 reflected. The FRA
 395 track class designation of “X” for “excepted” has a speed limit of 10 miles-per-hour (mph) but

396 excludes the exclusion of passenger trains. Therefore, an ordinal value of 0 replaced the “X”
 397 track class.

398 The railroad class (“CLASS_RR”) attribute encoded inconsistent values for “Class 1” where
 399 some labels were “1” and others were “1L” so the cleaning procedure ensured that attribute
 400 values ranged from 1 to 6. The railroad class is a ranking based on their annual operating revenue
 401 [1]. Therefore, the procedure re-interpreted the railroad class as an ordinal attribute. Table 5
 402 summarizes the results of the feature engineering procedure.

403 Table 5: Summary of Feature Engineering

Attribute	Procedure
CWR	Renamed SSB1 to CWR (continuously welded rail); binarized as “1” = “CWR” and “0” otherwise.
LOADED1	Binarized as “1” = “Y” (first involved car loaded?) and “0” = “N” for non-empty values.
WEATHER	Recoded nominal values in WEATHER as labels {Clear, Cloudy, Rain, Fog, Sleet, Snow}
TRK_TYP	Renamed TYPTRK (track type) and labeled nominal codes as {Main, Yard, Siding, Industry}
VISION	Renamed VISIBLTY and replaced nominal codes as descriptive {Dawn, Day, Dusk, Dark}
CLASS_RR	Renamed TYPRR (railroad class) and cleaned to contain only values from 1 to 6.
CLASS_TRK	Renamed TRKCLAS (track class) and cleaned to contain ordinal values from 0 to 9 (X → 0)
CONSIST	Renamed TYPEQ (consist type); repackaged as {freight, passenger, locomotive, cars, work, yard}. {1} → “Freight”, {2, 3, B, C} → “Passenger”, {8, D, E} → “Locomotive”, {5, 6} → “Cars”, {4, 9, A} → “Work”, {7} → “Yard”
ACC_TYPE	Renamed TYPE (accident type); repackaged as category labels: {1} → “Derail”, {2, 3, 6} → “Collide”, {4} → “Collide (Side)”, {5} → “Collide (Rake)”, {7, 8} → “RGC”, {9} → “Obstruct”, {10, 11} → “Fire”, {12, 13} → “Other”
MOVEx	Renamed MOPERA; repackaged as labels {signal, control, restrict, blocks, not main} {1, D} → “Signal”, {2, A, B, C, P} → “Control”, {3, L, M, I} → “Restrict”, {4, E, F, G, H, J, K} → “Blocks”, {5, N, O} → “Not Main”

404

405 **4.1.3 Data Imputation**

406 Table 6 summarizes the results of the imputing missing values and the impact of each method.

407 Table 6: Summary of Data Imputation

Attribute	Missing Before	Missing After	Procedure (N = 29,297, V = 49, M = 3)
TRK_DEN	51% (15,176)	0% (0)	Pivot STATION by TRK_TYP, aggregated as maximum TRK_DNSTY (track density). Fill missing data associated with the track type if defined, otherwise use the maximum value.
SIG	22% (6,473)	0%, 0	Pivot STATION by TRK_TYP, aggregated as net count SIGNAL (signalized territory). Fill missing data as “1” if net count associated with the track type is greater than 0, otherwise fill with “0”
CONSIST	39% (11,537)	8% (2,605)	Layer 1: Fill missing CONSIST with: “Freight” if (LOADF1 + EMPTYF1) > 0 otherwise “Passenger” if (LOADP1 + EMPTYP1) > 0 or PASSTRN is “Y”
	8% (2,605)	2% (844)	Layer 2: Fill missing CONSIST with: “Freight” if CLASS_RR is “1” (except “Amtrak”) otherwise “Passenger” if RAILROAD (reporting railroad) is “Amtrak”
	2% (844)	1% (377)	Layer 3: Fill missing CONSIST with: “Work Train” if TRK_TYP is not “Main”
	1% (377)	0% (0)	Layer 4: Fill missing CONSIST with: “Work Train” if TONS (gross tons, excluding locomotives) is 0 otherwise fill missing CONSIST with “Freight” if TONS > 0
CWR	21% (6,378)	0% (0)	Fill missing values with “1” if TRK_TYP is “main” and “0” otherwise.
MOVEx	0% (518)	0% (0)	Fill missing MOVEx based on SIGNAL or TRK_TYP.
PASSTRN	6%, (2,049)	0% (0)	Fill missing PASSTRN based on CONSIST. Check original flag for consistency with the type CONSIST and the sum of freight and passenger cars (loaded or empty). Flip the flag accordingly.
CLASS_RR	0%, (37)	0% (0)	Fill missing CLASS_RR (railroad class) by internet search: BLF → 2, {DD, METC} → 3, CN → 1
TRK_TYP	0%, (15)	0% (0)	Fill missing TRK_TYP (track type) by inference from the metadata.
CLASS_TRK	0%, (25)	0% (0)	Fill missing CLASS_TRK (track class) by inference from the metadata.

408
409 For track density (TRK_DEN), the LAP method used the nearest station (STATION) as the
410 location attribute and track type (TRK_TYP) as the sub-location attribute. There were 4,722
411 unique station names that served as keys for data merging. For the signal (“SIG”) attribute, the
412 LAP method counted the net presence of signalized territories for each track type near the station
413 and assigned “1” if the value was greater than 0 and “0” otherwise. That is, the LAP method
414 voted for the likelihood that the territory near the station used signaling to control movements.

415 The imputation technique for the type of “CONSIST” attribute used four layers of rule-based
416 inference to fill in missing values. The first layer inferred freight or passenger consist based on

417 the number of freight and passenger cars, respectively, resulting in a reduction of missing values
418 from 39% to only 8%. The next layer inferred freight or passenger consist based on the railroad
419 class, resulting in a further reduction of missing values to only 2%. The next two layers imputed
420 the remaining missing values by inferring the type of consist from the railroad class, the tonnage
421 hauled, and the track type.

422 Imputing missing values for the type of rail (“CWR”) used the probability that “main” track
423 types were continuously welded. A distribution of track type by CWR revealed that “main” track
424 types were more likely to be CWR than other track types. The probabilistic inference method
425 also filled the remaining movement type (“MOVEx”) and flag for passenger train
426 (“PASSTRN”). Evaluation of the metadata and an internet search filled the few remaining
427 missing values for track type and track class. Finally, there were no missing values.

428 ***4.1.4 Geospatial Cleaning***

429 Table 7 chronicles the progress of filling missing geospatial coordinates in each step of the
430 procedure. The LAP method filled missing values with the mean value of the non-zero latitude
431 and longitude values for that track type near the station, otherwise the method used the maximum
432 value. Subsequently a GIS spatial join revealed that 21.8% of the records had erroneous
433 geospatial coordinates because their locations on the map did not match the counties reported for
434 the accidents. Hence, the procedure replaced their geospatial coordinates with those of the
435 centroid for the FRA recorded county. There were a few missing county codes that the procedure
436 could not merge, so an internet search filled those missing values based on the station name.

437 Table 7: Chronicle of Geospatial Coordinate Cleaning

Attribute	Missing Before	Missing After	Procedure (N = 29,297 records)
Latitude	21% (6,415)	2% (817)	Treat zero-filled values as missing. Pivot STATION by TRK_TYP, aggregated as the average geospatial coordinate. Fill missing data with the mean value associated with the track type if available, otherwise fill with the maximum value.
Longitude	21% (6,415)	2% (820)	Treat zero-filled values as missing. Pivot STATION by TRK_TYP, aggregated as the average geospatial coordinate. Fill missing data with the mean value associated with the track type if available, otherwise fill with the <i>minimum</i> value (Longitude is negative in U.S.)
REC_ID	100%	0% (0)	Add a record identifier as the row index. V: 49+1=50 M: 3.
Latitude	2% (817)	0% (6)	Merge the FRA records with the TIGER® county shapefile by the FIPS5 code. Retain the geospatial centroid coordinates for each county. Add the state name abbreviation and flag (MATCH) to the attributes. V: 50+2=52. Add the county name and state name strings to the metadata. M: 3+2=5. Fill missing FRA geospatial coordinates with the county centroid coordinates.
Longitude	2% (820)	0% (6)	
Latitude	0% (6)	0% (0)	Manually fill missing geospatial coordinates for counties in Alaska and Florida.
Longitude	0% (6)	0% (0)	
FIPS5	0% (4)	0% (0)	Fill in missing FIPS5 codes for “Baltimore” and “Skagway” stations.
LAT	0% (0)	0% (0)	Rename Latitude to LAT and Longitude to LON after the geospatial cleaning procedure.
LON	0% (0)	0% (0)	

438

439 **4.1.5 Data Extraction**

440 Table 8 chronicles the reduction of data and attributes after the data extraction process.

441 Table 8: Chronicle of Data Reduction after Data Extraction

Attribute	Statistic	Procedure
ACC_CAT	N: 29,297 V: 52+1=53 M: 5	Add accident category: {Track, Equipment, Human, Signal, Miscellaneous}.
PASSTRN	N: 26,943 (92%) V: 53-4 = 49 M: 5	Dropped accidents involving passenger type trains. Dropped associated attributes: LOADP1, LOADP2, EMPTYP1, EMPTYP2.
DERAILED	N: 26,943 (92%) V: 49+1 = 50 M: 5	Added “Derailed” as the target attribute.
	N: 25,035	Dropped records where the accident cause was missing, 7% (1908)
	N: 15,088	Dropped records where human factors were a cause, 39.7% (9947)
	N: 15,087	Dropped 1 record with a missing value for WEATHER.

442

443 The statistics shown in the table are the number of records (N), number of attributes or variables

444 (V), and number of metadata fields (M). The algorithm used the “PASSTRN” as a flag to drop

445 records of accidents involving only passenger trains. Adding an accident category
 446 (“ACC_CAT”) flag helped the data extraction code to drop records of accidents caused by
 447 human factors. Adding the target attribute “DERAILED” indicated if the accident was a
 448 derailment type or not, and it became the label for supervised ML.

449 **4.1.6 Attribute Transformation**

450 Table 9 chronicles the transformation of attributes and their effect on feature reduction.

451 Table 9: Chronicle of the Transformed and Derived Attributes

Attribute	Reduction	Procedure
HR24	$50-3+1 = 48$	Combined TIMEHR, TIMEMIN, AMPM to 24-hour continuous, then drop old.
TRK_DEN_LG	$48-1+1 = 48$	Log Transform: TRK_DEN, then drop old.
TRNSPD_LG	$48-1+1 = 48$	Log Transform: TRNSPD, then drop old.
TONS_LG	$48-1+1 = 48$	Log Transform: TONS, then drop old.
POS_CAR	$48+1-1 = 48$	Rename and recode POSITON1 (position of first involved car) as the fractional position relative to the number of cars. 0 is front, 1 is back.
N_CARS	$48+1 = 49$	Add N_CARS as the sum of loaded and empty cars.
CARS_LD	$49+1-4 = 46$	Add CARS_LD as proportion of N_CARS loaded. Drop: LOADF1, EMPTYF1, POSITON1, PASSTRN
CARS_HZMT	$46+1-1 = 46$	Add CARS_HZMT as proportion of CARS_LD that carry Hazmat. Drop CARS (number of cars carrying hazmat)
SPD_OVR	$46+1-1 = 46$	Add to capture difference in train speed and speed limit for CLASS_TRK. Dropped field HIGHSPD.
Metadata	$46-6= 40$	Converted 6 attributes (REC_ID, SC, STATION, RAILROAD, RR3, IYR) to metadata: $5+6=11$.

452
 453 The procedure combined the three attributes related to time into a single attribute (HR24) that
 454 represented the hour as a continuous value within the range [0, 24). The combined attributes
 455 were hour (“TIMEHR”), minute (“TIMEMIN”), and AM flag (“AMPM”). The shifted log
 456 transformations reduced the skew of the track density (“TRK_DEN”), train speed (“TRNSPD”),
 457 and tonnage hauled (“TONS”) attributes. The three proportional transformations were relative to
 458 the number of cars (N_CARS), derived from the sum of loaded and empty cars. The
 459 “SPD_OVR” attribute was the excess train speed relative to the speed limit for the track class
 460 operated on. Hence, the value was negative for trains that were operating below the speed limit.
 461 Finally, the transformation procedure identified six attributes as irrelevant to the target and
 462 converted them to metadata. Examples were the state code (“SC”), station name (“STATION”),

463 railroad name (“RAILROAD”), track maintenance organization (“RR3”), and the incident year
464 (“YR”).

465 **4.1.7 Feature Selection**

466 Table 10 chronicles the feature reduction after eliminating post-event attributes. Table 11
467 summarizes the final set of 25 attributes used to build the ML models. The ML did not use the 11
468 metadata fields, but they supported further descriptive analysis. One-hot-encoding the categorical
469 attributes increased the number of features from 25 to 51. The dispersion indicates the amount of
470 variability in the distribution of each attribute. The dispersion measure is the *entropy* and
471 coefficient of variation (CV) for categorical and numerical attributes, respectively. The entropy
472 of an attribute is

$$H(X) = - \sum_{i=1}^N P(x_i) \log P(x_i) \quad (2)$$

473 where x_i is the i^{th} category value and $P(x_i)$ is a probability estimate based on their frequency of
474 occurrence in the dataset. For numerical attributes, the CV was the ratio of the standard deviation
475 to the mean value.

476

477 Table 10: Chronicle of the Eliminated Attributes

Attribute	Reduction	Process
POSCAR	40-1 = 39	Relative position of the first involved car in the train.
LOADED_1	39-1 = 38	Boolean: Is first involved car loaded? Missing (22%, 6568)
ACCDMG	38-1 = 37	Total reported damage in U.S. dollars.
CASKLD	37-1 = 36	Total killed for all involved railroads.
CASINJ	36-1 = 35	Total injured for all involved railroads.
CARSHZD	35-1 = 34	Number of cars that released hazardous materials.
CARSMDG	34-1 = 33	Number of cars damaged or derailed.
POSITON2	33-1 = 32	Position of car on the train that caused the accident.
EMPTYF2	32-1 = 31	Number of empty freight cars that derailed.
LOADF2	31-1 = 30	Number of loaded freight cars that derailed.
HEADEND2	30-1 = 29	Number of headend locomotives that derailed.
ACC_TYPE	29-1 = 28	Type of accident. Missing (0%, 83).
ACC_CAT	28-1 = 27	Accident cause category.
CAUSE	27-1 = 26	Accident cause code.
MATCH	26-1 = 25	Temporary geospatial filter flag for county mismatch.

478

479 Table 11: Summary of the ML Attributes, their Dispersion, and Type

Attribute	Dispersion	Type	Description (N=15,087, V=25, T=1)
DERAILED	0.631	Categorical	Target attribute: 1 if the accident type was derailment.
REGION	0.400	Categorical	Cleaned FRA region code for accident location.
LAT	0.133	Continuous	Cleaned latitude coordinate
LON	-0.126	Continuous	Cleaned longitude coordinate
CLASS_RR	0.796	Ordinal	Cleaned railroad class.
MONTH	0.549	Ordinal	Incident month.
DAY	0.561	Ordinal	Incident day.
HR24	0.541	Continuous	Transformed time to fractional 24-hour.
TEMP	0.391	Continuous	Temperature (degrees Fahrenheit)
VISION	1.110	Categorical	Visibility: {Dawn, Day, Dusk, Dark}
WEATHER	0.977	Categorical	Weather: {Clear, Cloudy, Rain, Fog, Sleet, Snow}
TRK_TYP	1.050	Categorical	Track Type: {Main, Yard, Siding, Industry}
TRK_CL	0.753	Ordinal	Track Class: {X as 0, 1 through 9}
CWR	0.685	Binary	1 if the rail type was continuously welded, 0 otherwise.
MOVE _x	1.250	Categorical	Movement: {Blocks, Control, Signal, Not Main, Restrict}
TRK_DEN_LG	0.972	Continuous	log(1+x) of annual track density in millions of gross tons.
SIG	0.590	Binary	1 if used signals to control train movements, 0 otherwise.
TRNSPD_LG	0.589	Continuous	log(1+x) of train speed in miles per hour (mph).
SPD_OVR	-1.304	Continuous	Difference between train speed and limit for track class.
CONSIST	0.950	Categorical	Consist: {Freight, Locomotive, Cars, Work, Yard}
TONS_LG	0.757	Continuous	log(1+x) of gross tonnage, excluding power units.
LOCOS	0.704	Ordinal	Number of headend locomotives.
N_CARS	0.915	Ordinal	Total number of cars.
CARS_LD	0.704	Continuous	Proportion of the number of cars that were loaded (0 to 1)
CARS_HZMT	2.800	Continuous	Proportion of loaded cars carrying hazardous materials (0 to 1)
HUMANS	0.562	Continuous	Number of humans present on the train.

480

481 **4.1.8 Outlier Removal**

482 Table 12 summarizes the AUC performance metric for a random forest classifier after removing
483 outliers using each of the four methods, with the various hyperparameter selections shown. All
484 algorithm and parameter selection produced similar performance. The framework used the LOF
485 algorithm with 20 nearest neighbors and 1% outliers because of its slight AUC performance
486 edge. The method removed 126 outliers to result in $15,087 - 126 = 14,961$ records used to train
487 and evaluate the ML models.

488 Table 12: Outlier Algorithm Performance Evaluation

Algorithm	Hyperparameters	AUC
One class SVM	Nu: 1%, Kernel Coefficient: 0.01	0.881
One class SVM	Nu: 1%, Kernel Coefficient: 0.1	0.878
One class SVM	Nu: 10%, Kernel Coefficient: 0.01	0.879
Local Outlier Factor	C: 1%, Neighbors: 10, Euclidean	0.879
Local Outlier Factor	C: 1%, Neighbors: 20, Euclidean	0.882
Local Outlier Factor	C: 1%, Neighbors: 50, Euclidean	0.880
Isolation Forest	C: 0%	0.881
Isolation Forest	C: 1%	0.880
Isolation Forest	C: 5%	0.880
Covariance Estimator	C: 1%	0.817

489

490 **4.2 Machine Learning**

491 Table 13 summarizes the stabilized performance of each ML algorithm, sorted by the AUC
492 metric. The null model is a no-skill model that predicts the dominant class each time. It provided
493 a baseline to compare the performance score of skilled classifiers. As expected, the CA score for
494 the no-skill classifier reflected the class imbalance of 67.42% for derailment type accidents
495 versus non-derailment type accidents. However, the AUC performance of the null classifier was
496 lowest as expected.

497 Tracking the AUC trend with 10-fold cross validation and stratified sampling produced the
498 optimum hyperparameter values shown in the table. Hyperparameters with common names

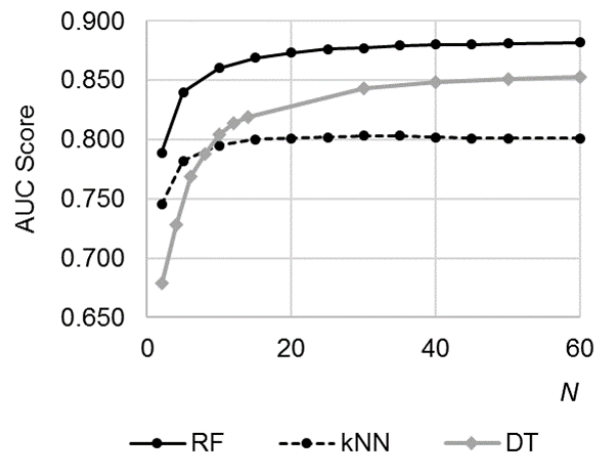
499 across some models were the learning rate (L), loss function (LF), regularization (R) parameters,
 500 and optimizer algorithm (OA).

501 Table 13: Model Performance and Optimum Hyperparameter Settings

Model	AUC	CA	F1	PR	RC	Optimum Hyperparameters
XGB	0.888	0.828	0.875	0.859	0.892	$\gamma:0$, Max Depth: 6, Min Child Weight: 1, R:1, w:1, L:0.2,
GB	0.884	0.824	0.872	0.854	0.891	LF: LR, Trees (N): 100, L: 0.2, Min Samples Leaf: 1
RF	0.882	0.821	0.817	0.817	0.821	Trees (N): 60, Attributes/Split: 5, Min Subset: 5
DT	0.854	0.803	0.801	0.800	0.803	Max Depth: 10, Min Samples Leaf (N): 90, Min Subset: 5
ANN	0.838	0.786	0.785	0.784	0.786	Hidden Nodes: 100, Activation: ReLu, OA: Adam ($\alpha:10^{-4}$)
LR	0.832	0.783	0.777	0.777	0.783	R (L2, C:5)
SGD	0.828	0.783	0.776	0.776	0.783	LF: (LR, $\epsilon:1$), R: E.Net ($\alpha:10^{-5}$, 0.15), L: IVS ($\eta_0:10^{-2}$, $t:0.25$)
kNN	0.803	0.765	0.759	0.758	0.764	N : 30, Distance (Euclidean, Weights: Uniform)
NB	0.794	0.725	0.730	0.740	0.725	No parameters to tune
ADB	0.713	0.746	0.746	0.747	0.746	Trees (N): 50, LF: Linear, OA: SAMME.R, LR: 1.0
SVM	0.626	0.654	0.639	0.633	0.654	Kernel: Sigmoid, R (C:0.2, $\epsilon:1.0$)
Null	0.500	0.674	0.543	0.455	0.674	No parameters to tune

502

503 To demonstrate the effect of hyperparameter tuning, Figure 4 plots the AUC score for a range of
 504 hyperparameter N associated with RF, kNN, and DT.



505
 506

Figure 4: AUC score as a function of hyperparameter N .

507 As noted in Table 13, the hyperparameter N represents the number of trees of a RF, the minimum
 508 number of samples to retain in the leaves of a DT, and the number of nearest neighbors for the
 509 kNN algorithm. The asymptotic trend was similar for all hyperparameters tuned.

510 **4.3 Feature Ranking**

511 Table 14 shows the importance ranking of the first 30 features in their strength of association
 512 with the target class. The rank by each of the five scoring methods are correlated as indicated by
 513 their pairwise correlation coefficients listed in Table 15. The correlation ranges from 84.2% for
 514 the gini and chi-squared methods to 94.5% for the ANOVA and chi-squared methods.

515 Table 14: Feature Importance Ranking

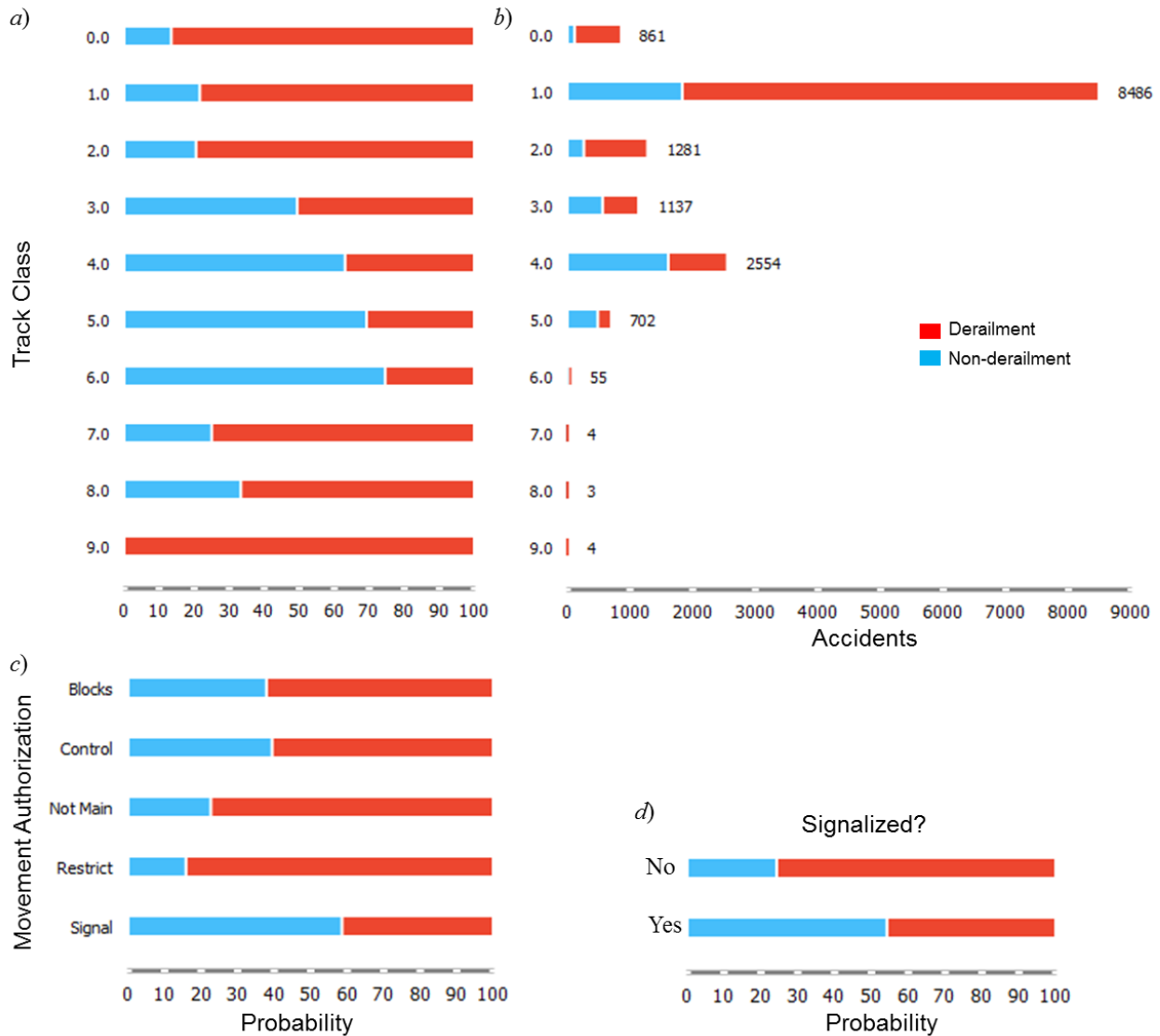
Feature	ANOVA	χ^2	Info. Gain	Gain Ratio	Gini
TRK_CL	1	2	4	3	2
MOVEx=Signal	2	3	3	1	4
SPD_OVR	3	1	7	11	3
SIG	4	4	5	2	5
HUMANS	5	7	6	10	6
TRK_TYP=Main	6	5	9	6	7
CWR	7	6	1	8	8
MOVEx=Not Main	8	11	11	9	11
LOCOS	9	9	10	12	9
CONSIST=Cars	10	8	14	4	12
TRK_TYP=Industry	11	10	12	7	14
TRK_TYP=Yard	12	16	2	18	16
TONS_LG	13	14	15	20	17
CARS_LD	14	18	13	19	13
CONSIST=Yard	15	15	18	17	19
N_CARS	16	12	28	16	10
MOVEx=Restrict	17	17	26	15	20
LAT	18	20	22	32	22
TEMP	19	22	24	30	21
TRK_TYP=Siding	20	21	25	13	24
VISION=Dark	21	24	21	24	25
CLASS_RR	22	13	30	14	15
TRK_DEN_LG	23	19	20	22	18
REGION=7.0	24	23	19	21	26
VISION=Day	25	31	29	35	27
REGION=8.0	26	26	27	23	28
REGION=6.0	27	27	23	28	29
REGION=2.0	28	28	33	25	30
TRNSPD_LG	29	25	37	5	1
REGION=3.0	30	29	31	31	31

516
 517 Figure 5 shows the probability distribution of derailment and non-derailment type accidents for
 518 the top two attributes (track class, movement authorization) and the fourth ranking attribute
 519 (signalized territory).

520 Table 15: Correlation of Ranking Methods

Method A	Method B	Correlation
ANOVA	Chi-Squared	0.945
ANOVA	Info. Gain	0.897
Gain Ratio	Gini	0.843
Gini	Chi-Squared	0.842

521



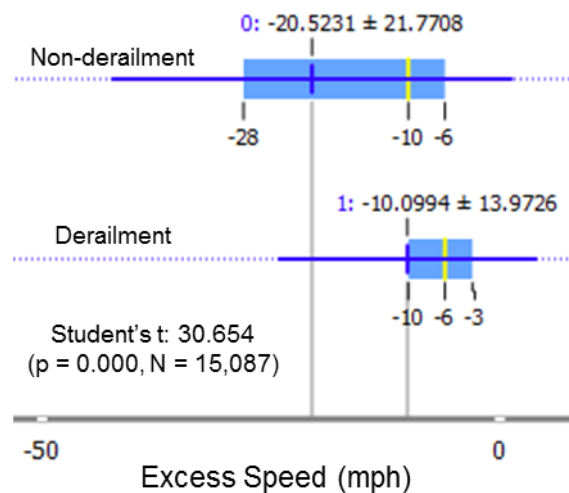
522
523

Figure 5: Class probability for the top two and fourth ranking attributes.

524 The distributions show that these attributes have some power to separate derailment from non-
525 derailment type accidents, but with uncertainty based on the amount of overlap in their class
526 distributions. For example, the class probability was higher for derailment type accidents on

527 class 0, 1, 2, 7, 8, and 9 tracks (Figure 5a). The distinction is significant for class 1 tracks
 528 because it has the highest frequency of occurrence (Figure 5b). Similarly, the class probability
 529 was higher for derailment type accidents where movement authority was within restricted limits
 530 (restricted) or where movement was not on main tracks (Figure 5c). Similarly, the class
 531 probability was higher for derailment type accidents in non-signalized territories (Figure 5d).
 532 The probability difference was much lower for the lower ranking attributes, but taken together,
 533 they improve the ML classification performance.

534 Figure 6 is a box plot that shows the distribution and statistics of excess speed for derailment
 535 and non-derailment type accidents.



536
 537

Figure 6: Distribution and statistics for excess speed.

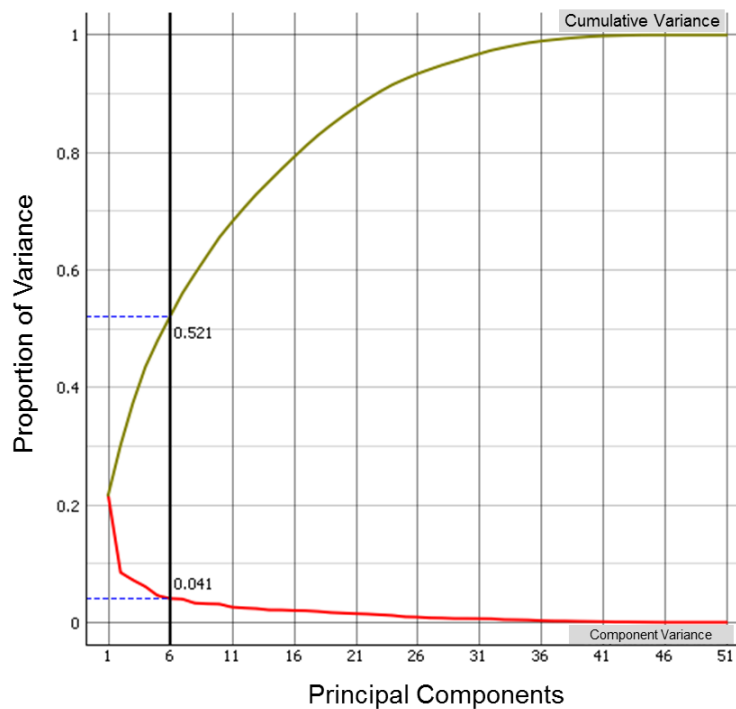
538 All accidents tended to occur below the speed limit for the track class on which they operated.
 539 However, derailment type accidents tended to occur closer to the speed limit than non-derailment
 540 type accidents. A student's t-test shows that the p-value was near zero, which indicated that the
 541 mean difference of 10 mph (16 kph) was statistically significant. The highlighted boxes in the
 542 figure indicates the values of the first quartile (25%) through the third quartile (75%) of the

543 dataset. The solid vertical and horizontal lines indicate the mean and standard deviation,
544 respectively. The lighter solid vertical lines indicate the median values.

545 4.4 Principle Component Analysis

546 Figure 7 plots the proportion of variance in the data that each PC explained. The top and bottom
547 curves show the cumulative variance and component variance explained, respectively, as a
548 function of each addition PC in their ranked order. This analysis indicated that the first six PCs
549 explained just over half of the variance in the dataset. Each of the remaining 45 of 51 total PCs
550 incrementally explain less than 4% of the variance each, but together account for the remaining
551 half of the variance explained.

552



553
554

Figure 7: The proportion of variance in the data that each PC explains.

555 Figure 8 and Figure 9 are visualizations of the PC clusters that suggest structure and noise in the
556 dataset.

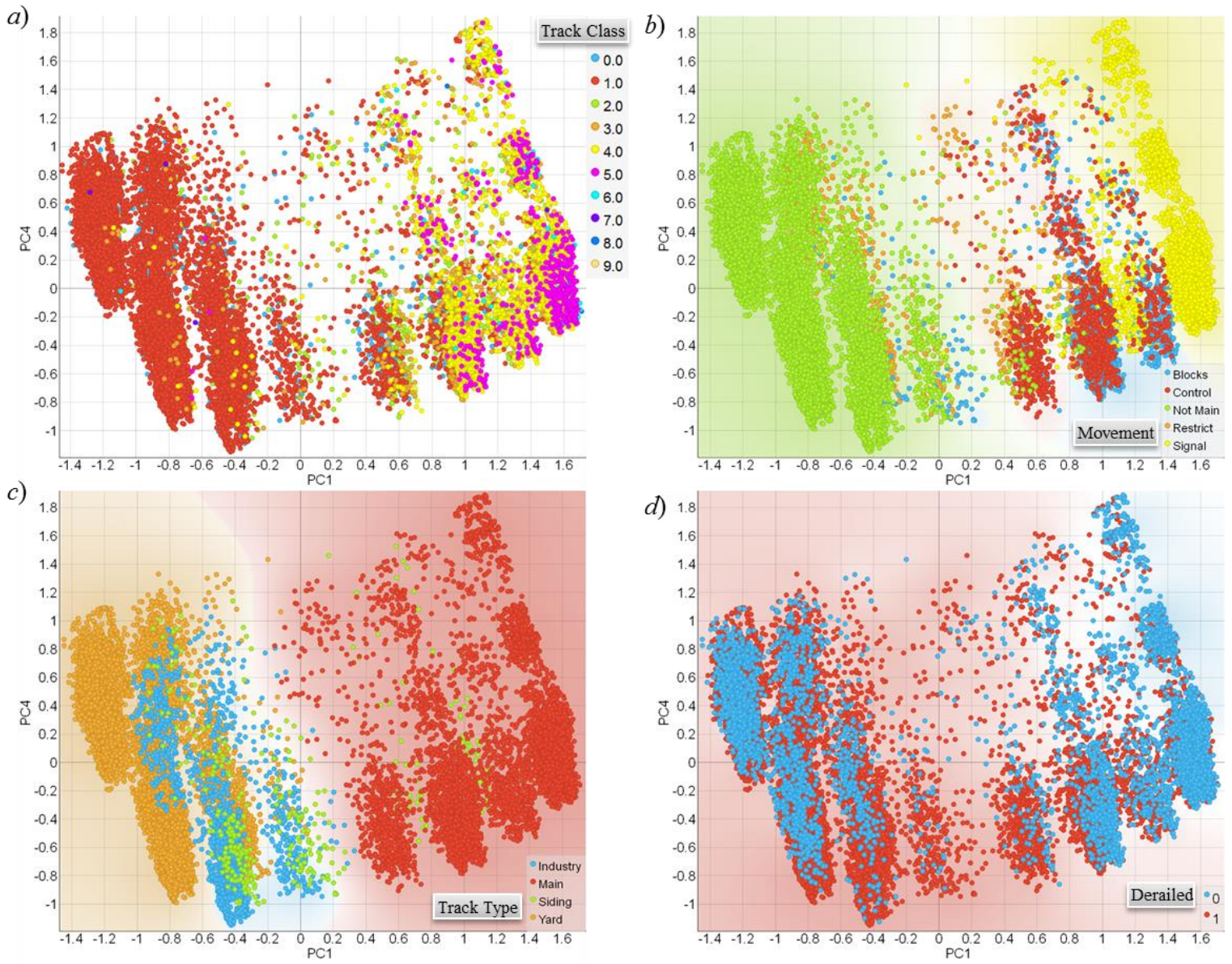


Figure 8: Data clusters for attributes with high power to distinguish among the target classes.

557
558

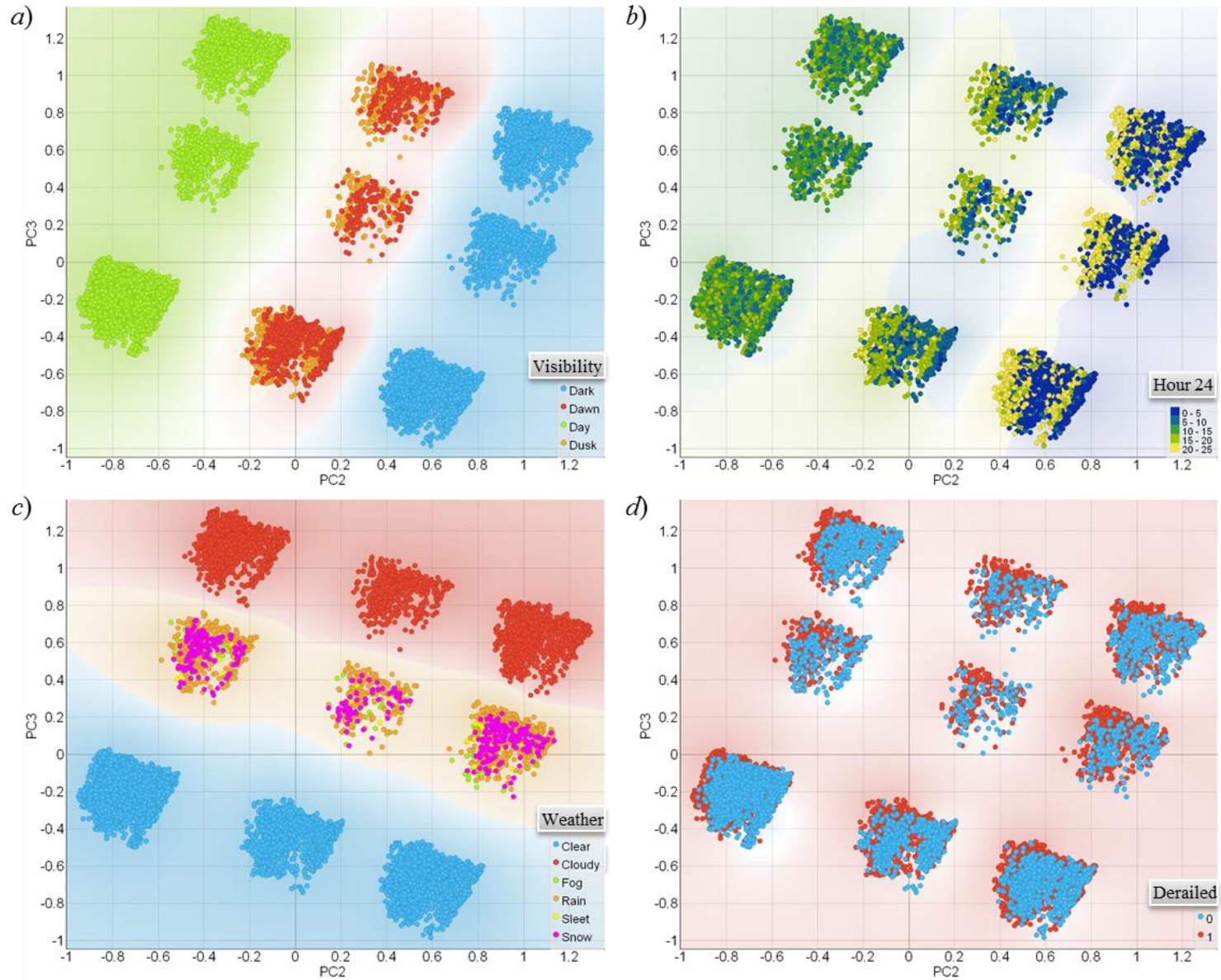


Figure 9: Data clusters for attributes with low power to distinguish among the target classes.

561 Figure 8 shows that PC1 and PC4 form elongated elliptical clusters for the top ranking attributes
562 of track class (Figure 8a), movement authority (Figure 8b), and track type (Figure 8c). Figure 8d
563 shows the distribution of the target class in the same PC feature space, where the color shading
564 indicates a bias towards the left clusters with negative PC1 values.

565 Figure 9 shows that PC2 and PC3 form nine distinct clusters for visibility (Figure 9a), hour
566 (Figure 9b), and weather (Figure 9c). Figure 9d shows the distribution of the target class across
567 each cluster. The clusters of the higher-ranking attributes (Figure 8) are less distinct than those of
568 the lower ranking attributes (Figure 9), which is further discussed for interpretation in the next
569 section.

570 **5 Discussion**

571 The overall good performance of the top four ML methods supported the effectiveness of the
572 custom data cleaning procedures, including the LAP technique introduced for imputing missing
573 values. The LAP method was most effective in filling missing values for track density, but that
574 attribute ranked low in importance for classification. Although effective, one limitation of the
575 LAP technique is that it provided a coarse imputation of the geospatial coordinates, based on an
576 aggregation of entries from other records where a value was present for the track type near that
577 station. However, in lieu of an alternative, the LAP imputed values to enable the operation of all
578 ML methods. The geospatial join method provided the next best alternative to replace erroneous
579 or low-resolution geospatial data. The distinctive southeast skew pattern revealed those records
580 with low-resolution data entry.

581 The top four algorithms of XGB, GB, RF, and DT were all based on the theories of decision
582 trees. They all achieved an AUC score greater than 85%. The highest AUC score of nearly 89%
583 for XGB was associated with a classification accuracy and balanced precision-recall scores (F1)

584 of nearly 83% and 88%, respectively. All methods were sensitive to hyperparameter tuning as
585 demonstrated in the performance improvement trends of Figure 4. The hyperparameter tuning
586 sensitivity cautions against using the default values suggested for each method.

587 All feature ranking methods and PCA pointed to track class (TRK_CL), signalized
588 movement authority (MOVEx = Signal), speed excess, and signalized territory (SIG) as the most
589 important features in ML classifier performance. The interpretation of an attribute rank is its
590 relative power to separate the distributions of the categories in the target class. That is, an
591 exceptionally high overlap of the two class distributions ranked the attribute exceptionally low in
592 importance towards classifier performance. It is rare that any one attribute can completely
593 distinguish among class members with 100% accuracy, otherwise there would be no need to use
594 additional attributes as explanatory factors for classification. Rather, a combination of attributes
595 contributes their ability to help determine the probability of class membership. Poor
596 classification results with all types of classification models may indicate that all attributes have a
597 high degree of overlap in their class probability distributions.

598 The PCA result (Figure 7) shows that the first 6 PCs explain more than half the variance in
599 the dataset but that it takes the remaining PCs, which accounted for 88% of the PCs, to explain
600 the remaining half of the variance in the data set. This outcome indicates that the first six PCs
601 represented the bulk of the information in the dataset. By extension, the remaining PCs likely
602 account for noise in the dataset based on the slow accumulation of the variance they explained.
603 This result suggests that just under half of the variance in the dataset lack structure and,
604 therefore, constitutes the noise in the dataset.

605 Figure 8 further illustrates structure in the dataset by clusters formed from PC1 and PC4 for
606 the top-ranking features of track class, movement authority, and track type. One can visualize the

607 amount of noise by the amount of attribute contamination of clusters and isolation from clusters.
608 Even though the target class was spread across all clusters (Figure 8d) there was an observable
609 bias of derailment type accidents towards clusters on the left. The bias corresponds to clusters of
610 class 1 tracks (Figure 8a), movement authorities not on the mainline (Figure 8b), and non-main
611 track types (Figure 8c). This result suggests that features that align with the cluster where the
612 derailment class is biased associates more with derailment than non-derailment type accidents.

613 Figure 9 shows that PC2 and PC3 form clusters for the attributes of visibility (Figure 9a),
614 hour (Figure 9b), and weather (Figure 9c), which are low-ranking. The even distribution of each
615 target class across each cluster (Figure 9d) agreed with their low importance ranking.

616 Interestingly, the level of isolation noise was much lower for those lower-ranking attributes. The
617 contamination noise in the center column of the cluster grid (Figure 9a) suggest similarities in
618 the visibility at dawn and dusk, as expected. Those similarities also corresponded to the
619 separation of “Hour 24” (Figure 9b) where day, night, and visibility transition times
620 corresponded to the expected hour ranges. The contamination in the center row of clusters of the
621 cluster grid (Figure 9c) suggest similarities in weather conditions like snow, sleet, rain, and fog.
622 Hence, the clustering results were as expected. The low level of isolation noise observed for the
623 clusters of the low-ranking features would have helped the ML performance more had the
624 situation occurred for the clusters of the highest-ranking features.

625 The above insights about the location of structure and noise in the dataset provided clues to
626 understand the reason for the performance differences of each ML method. Randomized tree-
627 based methods tend to train on various cross-sections of a dataset and use voting to determine the
628 class likelihood. In contrast, the other methods tend to leverage structure in the dataset. Hence,
629 the randomized tree-based methods such as XGB, GB, and RF performed better by discovering

630 patterns across noisy neighborhoods in dataset. On the other hand, kNN seeks local
631 neighborhoods to predict class membership based on attribute similarity. Consequently, noisy
632 neighborhoods can hamper classification performance as evidenced by the low performance rank
633 of kNN. Methods such as SVM and LR seek clear decision boundaries in multidimensional
634 feature space. Hence, the lack of clear hyperplanes between the target classes hampered their
635 performance. In fact, SVM achieved the lowest performance.

636 One limitation of the railroad accident database is that it does not necessarily list accidents
637 where the financial loss was below \$10,500 because the FRA does not require railroads to report
638 those. A second limitation is that the financial loss includes only the costs of repairing
639 equipment, signal systems, and infrastructure structures. Losses do not include costs associated
640 with cleanup, lost freight, societal damages, fatalities, injuries, and line closures. Nevertheless,
641 financial loss was not a pre-incident explanatory variable, but any future analysis that uses it
642 should be aware of this limitation in the dataset.

643 **6 Conclusions**

644 Railroads have been one of the most important modes of transport for more than a century.
645 Unfortunately, accidents continue to plague their operating safety and efficiency. Derailments
646 have consistently dominated other accident types and resulted in the greatest financial loss.
647 Therefore, gaining insights into factors that are more strongly associated with derailments than
648 other accident types can inform more cost-effective and impactful risk management strategies.

649 Recent advancements in computing capacity and their cost reduction has enabled machine
650 learning (ML) methods to uncover patterns in large multidimensional datasets that are difficult to
651 analyze with common rule-based and statistical methods. However, there are many types of ML
652 techniques, and no single method works best for all types of datasets. Therefore, this work

653 applied 11 different types of ML models to a large multidimensional dataset of railroad accidents
654 to compare their performance in predicting derailments from other accident types. The extreme
655 gradient boosting (XGB) classifier provided the best predictive performance with an AUC score
656 of 89%. The model could distinguish accident type with an accuracy of 83%. Principle
657 component analysis (PCA) revealed that high feature contamination noise and isolation noise
658 would prevent significant further gains in classification accuracy by any algorithm.

659 The good ML performance affirmed the relevance and sufficiency of the attributes in their
660 contribution towards distinguishing derailments from other accident types. Hence, knowing the
661 relative importance of those attributes towards classification accuracy can lead to insights for
662 decision-making in railroad risk management. The importance ranking used five different
663 methods that agreed on the ranking with correlations ranging from 84.2% to 94.5%. The
664 ANOVA and chi-squared methods agreed with the highest correlation that the top four attributes
665 were track class, the type of movement authority, the excess speed, and the presence of
666 signalization in the territory. The feature distribution for each target class and the PCA agreed
667 that relative to non-derailment type accidents, derailments were more strongly associated with
668 lower track classes, non-signalized territories, and movement authorizations with restricted
669 limits. Derailments also tended to occur at 10 mph (16 kph) below the speed limit of the track
670 class whereas non-derailment type accidents tended to occur at 20 mph (32 kph) below the limit.

671 The good ML performance also suggests that the custom data imputation techniques
672 presented were effective in filling missing values. The data-cleaning framework also
673 demonstrated a spatial join technique that addressed 21.8% of the geospatial data entry errors.
674 The detailed chronicle of the cleaning procedures will help other researchers save a substantial
675 amount of time in data preparation when using the same dataset. Future work will leverage the

676 framework to examine trends in accidents caused by human error to determine the effectiveness
677 of PTC deployments relative to historic accident rates.

678 **7 Data Availability**

679 This paper cited the sources of all the data used, which are currently publicly available.

680 **8 Conflicts of Interest**

681 The authors declare that there is no conflict of interest about the publication of this article.

682 **9 Credit**

683 Raj Bridgelall: conceptualization, methodology, software, data curation, formal analysis,
684 writing—original draft preparation. Denver Tolliver: supervision, resources, funding acquisition,
685 project administration, validation, writing—reviewing and editing.

686 **10 Funding Statement**

687 The authors conducted this work with support from North Dakota State University and the
688 Mountain-Plains Consortium, a University Transportation Center funded by the U.S. Department
689 of Transportation.

690 **References**

- [1] ASCE, "Infrastructure Report Card," American Society of Civil Engineers, Reston, VA, 2017.
- [2] R. Bridgelall and D. D. Tolliver, "Closed form models to assess railroad technology investments," *Transportation Planning and Technology*, vol. 43, no. 7, pp. 639-650, 2020.
- [3] Z. Zhang, X. Liu and K. Holt, "Positive Train Control (PTC) for railway safety in the United States: Policy developments and critical issues," *Utilities Policy*, vol. 51, no. 2018, pp. 33-40, 2018.
- [4] I. F. Ilyas and X. Chu, *Data Cleaning*, New York, NY: Association for Computing Machinery and Morgan & Claypool Publishers, 2019, p. 282.
- [5] M. Z. H. Jesmeen, J. Hossen, S. Sayeed, C. Ho, K. Tawsif, A. Rahman and E. Arif, "A Survey on Cleaning Dirty Data Using Machine Learning Paradigm for Big Data Analytics," *Indonesian Journal of Electrical Engineering and Computer Science*, vol. 10, no. 3, pp. 1234-1243, 2018.
- [6] R. Bridgelall, P. Lu, D. D. Tolliver and T. Xu, "Mining Connected Vehicle Data for Beneficial Patterns in Dubai Taxi Operations," *Journal of Advanced Transportation*, vol. 2018, pp. 1-8, 2018.
- [7] E. Rahm and H. H. Do, "Data Cleaning: Problems and Current Approaches," *IEEE Data(base) Engineering Bulletin*, vol. 23, pp. 3-13, 2000.
- [8] A. Iranitalab and A. J. Khattak, "Comparison of four statistical and machine learning methods for crash severity prediction.," *Accident Analysis & Prevention*, vol. 108, pp. 27-36, 2017.

- [9] F. Ghofrani, Q. He, R. M. Goverde and X. Liu, "Recent applications of big data analytics in railway transportation systems: A survey," *Transportation Research Part C-emerging Technologies*, vol. 90, pp. 226-246, 2018.
- [10] E. Dabbour, S. Easa and M. Haider, "Using fixed-parameter and random-parameter ordered regression models to identify significant factors that affect the severity of drivers' injuries in vehicle-train collisions.," *Accident Analysis & Prevention*, vol. 107, pp. 20-30, 2017.
- [11] J. Liu and A. J. Khattak, "Gate-violation behavior at highway-rail grade crossings and the consequences: Using geo-Spatial modeling integrated with path analysis.," *Accident Analysis & Prevention*, vol. 109, pp. 99-112, 2017.
- [12] A. Keramati, P. Lu, A. Iranitalab, D. Pan and Y. Huang, "A crash severity analysis at highway-rail grade crossings: The random survival forest method.," *Accident Analysis & Prevention*, vol. 144, p. 105683, 2020.
- [13] S. Soleimani, S. R. Mousa, J. Codjoe and M. Leitner, "A Comprehensive Railroad-Highway Grade Crossing Consolidation Model: A Machine Learning Approach.," *Accident Analysis & Prevention*, vol. 128, pp. 65-77, 2019.
- [14] B. Wali, A. J. Khattak and N. Ahmad, "Injury severity analysis of pedestrian and bicyclist trespassing crashes at non-crossings: A hybrid predictive text analytics and heterogeneity-based statistical modeling approach," *Accident Analysis & Prevention*, vol. 150, p. 105835, 2021.
- [15] X. Liu, M. R. Saat and C. P. Barkan, "Freight-train derailment rates for railroad safety and risk analysis.," *Accident Analysis & Prevention*, vol. 98, pp. 1-9, 2017.
- [16] B. Z. Wang, C. P. L. Barkan and M. R. Saat, "Quantitative Analysis of Changes in Freight Train Derailment Causes and Rates," *Journal of Transportation Engineering, Part A: Systems*, vol. 146, no. 11, p. 4020127, 2020.
- [17] A. Iranitalab and A. J. Khattak, "Probabilistic classification of hazardous materials release events in train incidents and cargo tank truck crashes," *Reliability Engineering & System Safety*, vol. 199, p. 106914, 2020.
- [18] H. Li, D. Parikh, Q. He, B. Qian, Z. Li, D. Fang and A. Hampapur, "Improving rail network velocity: A machine learning approach to predictive maintenance," *Transportation Research Part C-emerging Technologies*, vol. 45, pp. 17-26, 2014.
- [19] A. Lasisi and N. Attoh-Okine, "Machine Learning Ensembles and Rail Defects Prediction: Multilayer Stacking Methodology," *ASCE-ASME Journal of Risk and Uncertainty in Engineering Systems, Part A: Civil Engineering*, vol. 5, no. 4, p. 4019016, 2019.
- [20] K. P. Murphy, *Machine Learning : A Probabilistic Perspective*, Cambridge, Massachusetts: The MIT Press, 2012.
- [21] N. Z. Abidin, A. R. Ismail and N. A. Emran, "Performance Analysis Of Machine Learning Algorithms For Missing Value Imputation," *International Journal of Advanced Computer Science and Applications*, vol. 9, no. 6, 2018.
- [22] FRA, "Rail Equipment Accident/Incident Data File Structure and Field Input Specifications," Federal Railroad Administration (FRA), Washington, D.C., 2011.
- [23] W. G. Manning and J. Mullahy, "Estimating log models: to transform or not to transform?," *Journal of Health Economics*, vol. 20, no. 4, pp. 461-494, 2001.
- [24] F. T. Liu, K. M. Ting and Z.-H. Zhou, "Isolation-Based Anomaly Detection," *ACM Transactions on Knowledge Discovery From Data*, vol. 6, no. 1, p. 3, 2012.
- [25] P. J. Rousseeuw and K. V. Driessen, "A fast algorithm for the minimum covariance determinant estimator," *Technometrics*, vol. 41, no. 3, pp. 212-223, 1999.
- [26] M. M. Breunig, H.-P. Kriegel, R. T. Ng and J. Sander, "LOF: identifying density-based local outliers," in *Proceedings of the 2000 ACM SIGMOD international conference on Management of data*, 2000.
- [27] G. James, D. Witten, T. Hastie and R. Tibshirani, *An Introduction to Statistical Learning with Applications in R*, vol. 112, New York: Springer, 2013.
- [28] A. Géron, *Hands-On Machine Learning with Scikit-Learn and TensorFlow: Concepts, Tools, and Techniques to Build Intelligent Systems*, 2nd ed., Sebastopol, California: O'Reilly Media, 2017, p. 856.
- [29] T. Hastie, R. Tibshirani and J. Friedman, *The Elements of Statistical Learning: Data Mining, Inference, and*

Prediction, 2nd ed., New York, New York: Springer, 2016, p. 767.

- [30] T. Fawcett, "An introduction to ROC analysis," *Pattern Recognition Letters*, vol. 27, no. 8, pp. 861-874, 2006.
- [31] B. Krawczyk, "Learning from Imbalanced Data: Open Challenges and Future Directions," *Progress in Artificial Intelligence*, vol. 5, no. 4, pp. 221-232, 2016.
- [32] L. Yu and H. Liu, "Feature Selection for High-Dimensional Data: A Fast Correlation-Based Filter Solution," in *The Twentieth International Conference on Machine Learning (ICML-2003)*, Washington, D.C., 2003.
- [33] H. Wang, T. M. Khoshgoftaar and K. Gao, "A Comparative Study of Filter-Based Feature Ranking Techniques," in *2010 IEEE International Conference on Information Reuse & Integration*, Las Vegas, Nevada, 2010.
- [34] A. Agresti, *Statistical Methods for the Social Sciences*, 5th ed., Boston, Massachusetts: Pearson, 2018, p. 608.
- [35] J. R. Quinlan, "Induction of Decision Trees," *Machine Learning*, vol. 1, no. 1, pp. 81-106, 1986.
- [36] H. Han, X. Guo and H. Yu, "Variable Selection Using Mean Decrease Accuracy and Mean Decrease Gini Based on Random Forest," in *The 7th IEEE International Conference on Software Engineering and Service Science (ICSESS)*, 2016.
- [37] I. T. Jolliffe and J. Cadima, "Principal Component Analysis: A Review and Recent Developments," *Philosophical Transactions of the Royal Society A: Mathematical, Physical and Engineering Sciences*, vol. 374, no. 2065, p. 20150202, 2016.

691

692